Trends Phytochem. Res. 5(3) 2021 126-135

Trends in Phytochemical Research (TPR)

Journal Homepage: http://tpr.iau-shahrood.ac.ir

Original Research Article

Investigation of inhibitory properties of triphenyl-LasR enzyme involved in the quorum sensing of *Pseudomonas aeruginosa* by molecular modeling

MAHSHAD SHAHRIARI[1], FAEZEH NOURMANDIPOUR[1], SAMIRA NOROUZI[1] AND SAMAD NEJAD EBRAHIMI[1]✉*

[1]Department of Phytochemistry, Medicinal Plants and Drugs Research Institute, Shahid Beheshti University, Evin, Tehran, Iran

ABSTRACT

Quorum sensing (QS) is a bacterial communication mechanism that regulates the production of many pathogenic factors, including the formation of pigments and the ability to form biofilms that are essential for chronic infections. For discovering new inhibitors on the formation of biofilm formation, over 700 synthetic and natural compounds have been virtually screened against the triphenyl-LasR enzyme involved in *Pseudomonas aeruginosa's* QS system. The 3D-QSAR studies revealed the relationship between the quantitative structure of compounds and their activity. The drug-like properties of compounds and effective pharmacophore features on the ligand interaction with protein were investigated by ADME and E-pharmacophore analysis. According to the obtained results, we identified compound with PubChem ID 118732838 with the glide score of -12.34 kcal/mol and oral absorption of 58.75% as the potential compound for inhibiting triphenyl-LasR protein. The study outcomes can help us to identify new drugs to inhibit biofilm formation and decrease bacterial resistance.

ARTICLE HISTORY

Received: 29 May 2021
Revised: 27 June 2021
Accepted: 29 June 2021
ePublished: 25 September 2021

KEYWORDS

Biofilm formation
MM-GBSA
Molecular docking
Pharmacophore
QSAR
Quorum sensing

1. Introduction

The increase in bacterial resistance against conventional antibiotics has prompted researchers to develop new antibiotics with new targets and mechanisms. One mechanism that attracted attention was the identification of quorum sensing (QS). The QS is a cell-to-cell communication that monitors the density of the bacterial population to produce a biofilm, a viscous and adhesive layer (Pejin et al., 2017), which protects bacteria against attacks by immune cells and antibiotics (Pejin et al., 2014; Pejin et al., 2015a). The quorum-sensing mechanism is created by a small molecule signal called an autoinducer. When the autoinducer concentration exceeds beyond a limit, it binds to its receptor and activates the transcription of various genes involved in biofilm formation (Zou and Nair, 2009). In Gram-negative bacterium such as *Escherichia coli*, *Coccobacillus*, and *Pseudomonas aeruginosa*, QS is mediated by acyl-homoserine lactone (AHL), a signaling molecule that regulates the expression of biofilm formation genes (Aliyu et al., 2016). *P. aeruginosa* is an encapsulated Gram-negative bacteria that can cause infections in humans, especially those with a weak immune system. This bacterium in addition to having intrinsic and acquired resistance mechanisms, such as the low permeability of the external membrane, efflux pump expression, deactivating antibiotics, and achieving mutational changes, also possesses adaptive resistance where it forms biofilms to limit antibiotic access to bacterial cells (de Kievit et al., 2002; Pejin et al., 2015b). *P. aeruginosa* has two QS systems to form a biofilm, LAS and RHL. LAS system consists of Las-I (The enzyme acyl-homoserine lactone synthase (AHL synthase)) and LasR (Transcription activator protein) genes (de Kievit et al., 2002). LasR is the central regulator of the QS system, which belongs to the LuxR protein family and acts as a transcriptional activator

✉Corresponding author: Samad Nejad Ebrahimi
Tel.: +98 21 29904052, Fax: +98 21 22431783
E-mail address: s_ebrahimi@sbu.ac.ir, **doi: 10.30495/tpr.2021.1931857.1209**

(Kiratisin et al., 2002; O'Brien et al., 2015; Mizdal et al., 2018). When the AHL concentration is present at the allowable limit, LasR binds this signal and recruits transcriptional machinery to induce QS gene expression (Gerdt et al., 2014). Based on the vital role of LasR in biofilm formation, finding the appropriate antagonist of the LasR enzyme, like an AHL receptor, may prevent AHL from connecting with the protein and suppressing the synthesis of virulence factors and the formation of biofilms which make bacteria more vulnerable (Manson et al., 2020). Given that there is no selection pressure, it is unlikely that bacteria will develop multidrug resistance (Aliyu et al., 2016). Different *in vitro*, *in vivo*, and computational methods have been employed to assess the antibacterial potential of drugs or chemical compounds against *P. aeruginosa*. Amongst these methods, molecular docking is one of the short time computational methods which screen the available medications to identify potential drugs for new diseases and predict the adverse effects of novel drugs (Norouzi et al., 2021). For this purpose, we evaluated a virtual screening protocol for discovering new inhibitory among the more than 700 chemical compounds (Half natural and half semi-synthesis) obtained from PubChem against the triphenyl-LasR enzyme to develop potential antibiotics which can disrupt the LasR system.

2. Experimental

2.1. Computational details

The virtual screening based on docking studies was performed using the Glide and Induced fit docking (IFD) program in the Maestro 11.8 (Schrodinger, LLC). PHASE module executed E-pharmacophore modeling and 3D quantitative structure-activity relationship (3D QSAR) model (Maestro 11.8). The prediction of Absorption, Distribution, Metabolism and Excretion (ADME) properties and molecular mechanics-generalized born surface area (MM-GBSA) were carried out by QikProp and prime module in Maestro 11.8 (Fig. 1).

2.2. Ligand preparation

We downloaded over 700 chemical compounds (Half natural and half semi-synthesis) with inhibitory effects against *P. aeruginosa* from PubChem to select potent compounds with high inhibitory activity against the LasR enzyme to inhibit the QS system and decrease bacterial resistance. Conversion of their 2D to 3D structures was performed by LigPrep module with an OPLS3 force field through the Schrödinger 2018 suite package. The ionization state of ligands did not change, salts have

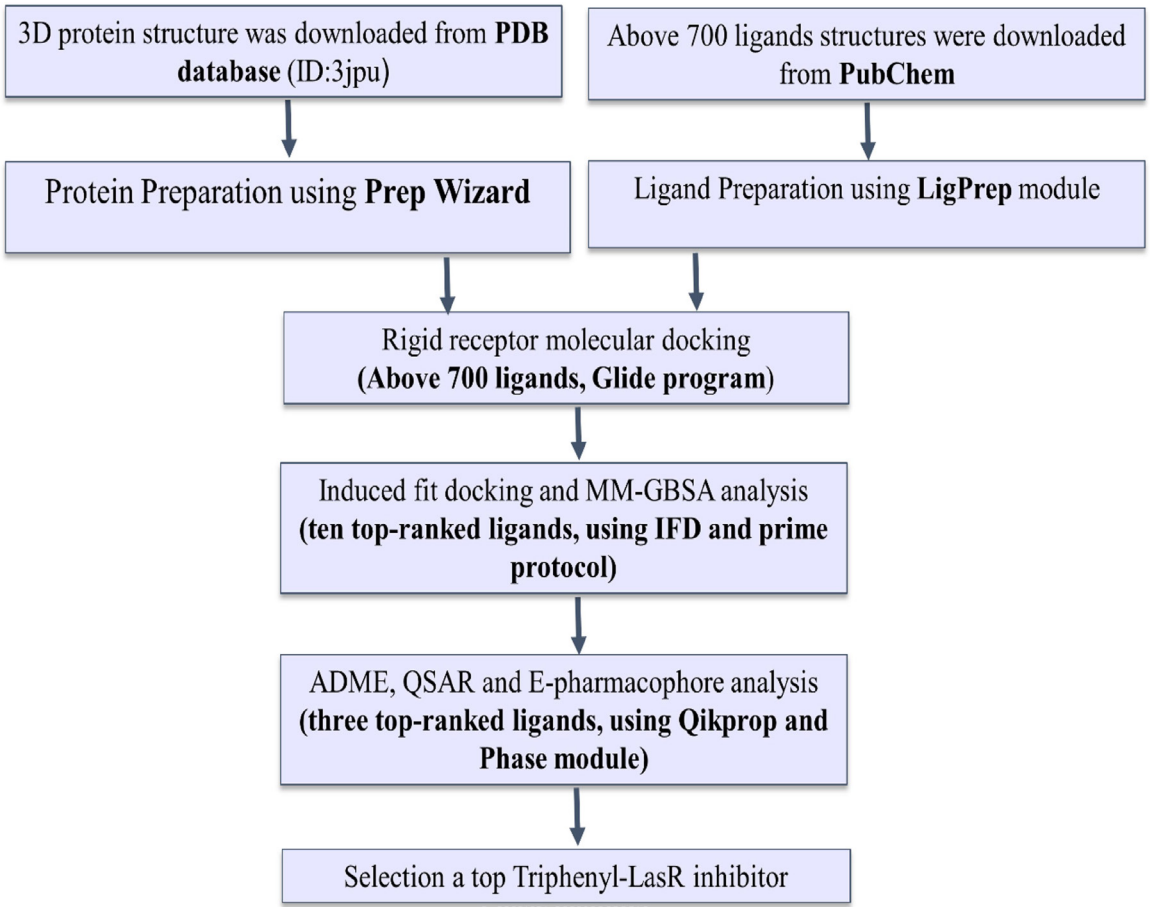

Fig. 1. Schematic representation of the docking procedure and analysis.

been removed, and no tautomers were considered. The stereoisomer computation was performed to determine chirality from 3D structures and generate at most 1 per ligand. The 3D conformers were developed based on ≤10 per rotatable bond and ≤100 per ligand, and the redundant conformers were removed based on the root mean square deviation (RMSD) cut-off value of 1.0 Å. Then, to eliminate high energy structures, each conformer was filtered through a relevant energy window of 10.0 kcal/mol.

2.3. Protein preparation

The X-RAY diffraction structure of triphenyl-LasR (PDB ID: 3JPU) with the structure resolution of 2.30 Angstrom (Å) was downloaded from the Protein Data Bank (PDB). The preparation of the protein structure was performed by the protein preparation wizard (Maestro11.8). In the Preparation process, the missing hydrogens were added, water molecules beyond 5 Å from the het-group were deleted, and ionization and tautomeric states were generated at the physiological pH range (7.0 ± 2.0) using Epik (Empirical pKa Prediction). Further, the unwanted chains and waters that are not important for ligand binding were deleted. The orientations of hydrogen-bonded groups were optimized at pH 7.0, and the corrected structures were minimized to relieve strain and tune the placement of various groups (Subhani and Jamil, 2015; Ganjoo and Prabhakar, 2019).

2.4. Glide docking

The rigid receptor docking was carried using the Glide program in Maestro 11.8. The Glide program predicts the binding affinity between the selected ligands and the active site of the enzyme. Amino acid residues Gly 126, Cys 179, Leu 110, Trp 88, Phe 101, Asp 173, Ile 52, Tyr 47, Ala 50 that are vital in the critical interactions in 6 Å distance between native ligand and protein were settled as the protein grid box for the protein grid generation module of the Glide program (Fuqua and Greenberg, 2002; Li and Nair, 2012). Ligands with 20Å length from each edge of the enclosing box were docked on extra precision (XP) mode in the OPLS3 force field. No limitations were applied for all the docking studies.

2.5. Induced Fit Docking (IFD)

Flexible protein-ligand docking to investigate some aspects of protein flexibility was performed using the Induced Fit Docking (IFD) application in Maestro 11.8. In the IFD approach, the receptor is not held rigid and can change its binding site more closely conformed with the ligand shape and binding mode (Kashyap and Kakkar, 2020). The binding site residues (Gly 126, Cys 179, Leu 110, Trp 88, Phe 101, Asp 173, Ile 52, Tyr 47, Ala 50), which represent protein functional sites, were determined as Box center, and 20 Å was determined as the length of each edge of the enclosing box. We set the receptor van der Waals scaling to 0.5 to allow better side-chain flexibility during docking. Residues below 5 Å from any ligand pose have been refined. Structures within 30.0 kcal/mol of the minimum energy structure were moved forward for redocking. Finally, extra-precision (XP) has been selected for the Glide redocking stage. The software calculates the IFD score according to the following (Subhani and Jamil, 2015):

$$IFDscore" = 1.0 \times Glidescore + 0.05 \times Prime\_Energy \quad \text{(Eqn.1)}$$

The best conformation for each ligand was selected based on IFD scores.

2.6. Prime molecular mechanics-generalized born surface area (MM-GBSA) calculations

The free binding energy of the protein-ligand complex was calculated using the MM-GBSA analysis via the Prime module in Maestro 11.8. The binding energy (ΔG bind) is calculated according to the following equation:

$$\Delta G_{bind} = E_{complex}(minimized) - [E_{ligand}(minimized) + E_{receptor}(minimized)] \quad \text{(Eqn. 2)}$$

$E_{Complex}$, E_{Ligand}, and $E_{Receptor}$ denote the optimized energy of the protein-ligand complex (complex), free ligand (ligand), and free receptor (receptor), respectively. Each energy term combines different energies such as Coulomb energy, van der Waals, covalent binding, lipophilic, Generalized Born electrostatic solvation, prime, hydrogen-bonding, and packing energy. The VSGB solvation model was used in the calculations (Chintha et al., 2020).

2.7. Atom-based 3D-QSAR model generation

The QSAR approach is a computational method that describes the relationship between the physicochemical characteristic of a specific structure and its biological activity through the pIC_{50} (the negative logarithm of the IC_{50} value) report (Al-Bagawi et al., 2020).

2.7.1. Dataset for LasR inhibitory activity

A dataset of previously reported potential compounds with LasR inhibitory activity on *P. aeruginosa* was downloaded from PubChem to generate an atom-based 3D QSAR model. Structures were minimized and optimized using the LigPrep module under the same conditions mentioned earlier. Biological activity (IC_{50}) was converted into the equivalent:

$$pIC_{50} = -\log(IC_{50}) \quad \text{(Eqn. 3)}$$

The calculated pIC_{50} was used as a dependent variable for the generation of the QSAR model (Vora et al., 2019). PubChem IDs of the chemical structures and experimental activity data are shown in Table 1.

Table 1
MM-GBSA and binding energy (in kcal/mol) between triphenyl-LasR and ligands.

Ligand. Nu	PubChem ID	Glide G score (kcal/mol)	MM-GBSA (kcal/mol)	IFD score (kcal/mol)
Nu-1	118732846	-12.42	-73.98	-365.76
Nu-2	118732838	-12.34	-94.75	-365.22
Nu-3	118732849	-12.32	-102.21	-365
Nu-4	118732840	-12.27	-92.1	-365.71
Nu-5	11177309	-12.26	-80.09	-359.64
Nu-6	72710969	-12.06	-95.11	-363.82
Nu-7	100313	-12.01	-96.04	-358.77
Nu-8	118732854	-11.95	-92.27	-365.43
Nu-9	118732847	-11.94	-72.94	-365.48
Nu-10	71817321	-11.86	-67.08	-362.65

2.7.2. 3D-QSAR model generation

Division of data into training and test sets is an essential step in QSAR analysis that is used to build the model and evaluate the predictive ability of the build model. In this study, to generate a 3D-QSAR model, the data were randomly split into 75% of training and 25% of test set molecules in the QSAR atom-based program (Maestro 11.8). The QSAR model was performed by taking three maximum PLS factors with three outliers. The test set of the dataset was used for external validation. Q^2 and RMSE values signify the predicted activity and root-mean-square error of test set molecules. Other statistical parameters such as R^2 scramble, the standard deviation of the regression (SD), F value, p-value, stability, and Pearson-R of the model's prediction were also calculated (Vora et al., 2019).

2.8. Lipinski's rule for drug likeliness and in silico ADME prediction

The ADME properties are essential factors to determine the drug-like properties of compounds. Most of the drug development projects fail in clinical trials due to poor ADME properties (Lucas et al., 2019). For this purpose, the drug likeliness and pharmacokinetic parameters of the selected compounds were predicted using the QikProp program in Maestro 11.8. This software can compare the particular molecule properties with those of 95% of known drugs. The physical and pharmacological properties of the structures, such as the human oral absorption, molecular weight, the number of hydrogen bond acceptors and hydrogen-bond donors, octanol/water partition coefficient log p, and the number of violations of Lipinski rule of five were predicted by ADME studies.

2.9. Generation of energy-optimized structure-based pharmacophores (E-pharmacophore) model

E-pharmacophore model was generated through the phase program of Maestro 11.8. IFD output file, obtained after docking of native ligand to the protein crystal structure, was used to create the E-pharmacophore. This program scores the various interactions that the ligand makes to the receptor during docking and then picks and prioritizes the possible pharmacophore features on the ligand that make those key interactions (Tripathi et al., 2016). Pharmacophore sites were automatically generated using the default set of six chemical features: hydrogen bond acceptor (A), hydrogen bond donor (D), hydrophobic (H), aromatic ring (R), negative ionizable (N), and positive ionizable (P).

2.10. Reference drug

Tobramycin is an FDA-approved drug that is used as first-line therapy in the treatment of P. aeruginosa infections (Akkerman-Nijland et al., 2020; Ho et al., 2020). For this purpose, the tobramycin is a positive control to investigated ADME properties of the selected compounds. The 2D structure of tobramycin was downloaded from PubChem (PubChem ID: 36294) and prepared with ligand preparation software using Maestro 11.8 in the same way as mentioned before. The ADME studies on tobramycin were done and used for comparison with selected ligands.

3. Results and Discussion

Discovering new compounds with QS inhibitory properties creates a significant breakthrough in the generation of antibacterial drugs for decreasing bacterial resistance mechanisms in *P. aeruginosa*. In this study, we used *in-silico* analysis techniques to simplify predicting a particular molecule as the potent lead compound for inhibiting LasR system of *P. aeruginosa*.

3.1. Method validation

We investigated the interactions between native ligand and best compound resulted from glide docking (PubChem ID: 118732846) with a glide score -12.42

kcal/mol for method validation. According to Fig. 2, the residues similarity around both ligands proves that they have interactions in the one receptor site with the protein. Based on this, it can be confirmed that the active site which has been chosen for forming the Grid box is correct, and the tested compounds had a good interaction with the receptor.

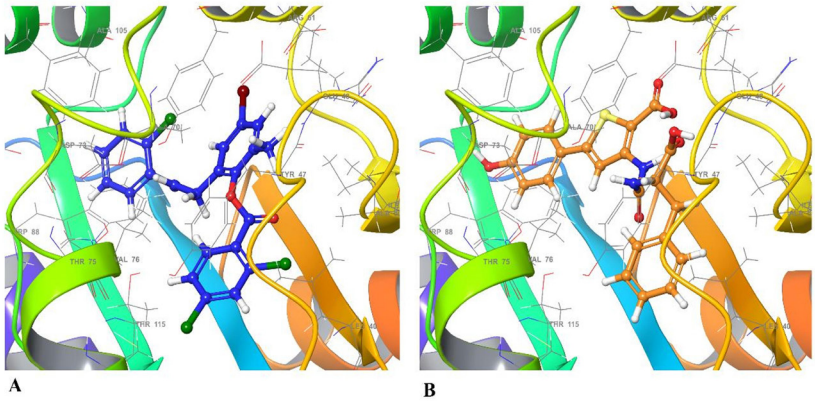

Fig. 2. Overlaying and comparison docking of (**A**) native ligand and (**B**) best compound with the highest glide score (PubChem ID: 118732846).

3.2. Docking analysis of triphenyl-LasR

3.2.1. Glide docking study

Initial docking in a simple manner with flexible ligand and rigid receptor approach was performed to determine the potent LasR inhibitor among more than 700 compounds which conclude half natural and half semi-synthesis compounds. The results showed that 51% of compounds showed a docking score in the range of -7 to -12 kcal/mol. The glide scores and 2D structures of ten top-ranked ligands, selected based on docking studies, are represented in Table 1 and Fig. 3.

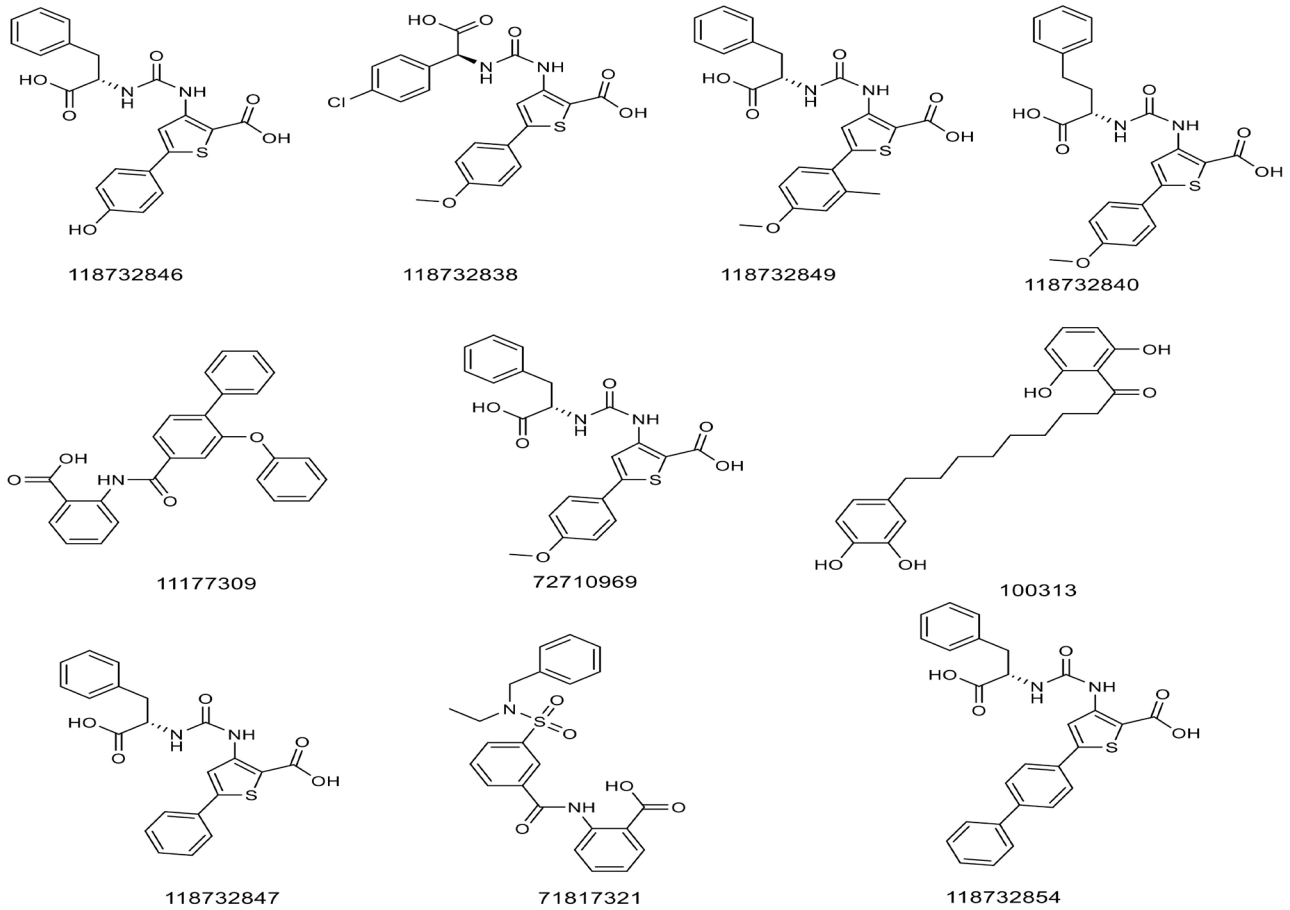

Fig. 3. The 2D structure and PubChem ID of the top 10 compounds showed the highest glide score with triphenyl-LasR enzyme.

Each compound has different functional groups in its structures, which affects its interaction with the protein's active site. Ligands Nu-1, Nu-2, Nu-3, Nu-4, Nu-6, Nu-8, and Nu-9 with glide score -12.42, -12.34, -12.32, -12.27, -12.06, -11.95, and -11.94 kcal/mol, respectively, have thiophene, urea, carboxylic acid, and benzene groups in their structure which have interactions with Tyr 47, Trp 60, Tyr 64, and Asp 65, respectively. Ligands Nu-5 and Nu-10 with glide score -12.26 and -11.86 kcal/mol have benzoic acid and amide group with showed interaction with Asp 73 and Ser 129. Ligand Nu-7 with glide score -12.01, which is known as Malabaricone C, is a diarylnonanoid that has been found in Myristica and has diverse biological activities. This compound showed interactions with Tyr 47 via benzene ring and with Leu 125, and Tyr 93 through phenolic hydroxyl groups. Generally, based on our glide docking study, the top ten compounds interact with the triphenyl-LasR protein using π-π stacking interactions with Tyr 47, and Tyr 64, and Hydrogen binding with Asp 56, Trp 60, Asp 73 and Ser 129. A brief description of the nature of the top ten compounds was investigated in Table 1.

3.2.2. Induced fit docking (IFD) study

Among the discovery of novel inhibitors based on computational techniques, IFD plays a vital role in understanding the molecular interactions between the ligand and active site of the protein. For this purpose, to consider both ligand and receptor flexibility, the IFD approach was investigated for ten ligands with more negative glide scores (Table 1). This process resulted in a preference of five ligands with PubChem ID 118732846 (Nu-1), 118732838 (Nu-2), 118732840 (Nu-4), 118732854 (Nu-8), and 118732847 (Nu-9) with IFD score in the range of -365.22 to -365.76 kcal/mol. Ligand Nu.1 showed hydrogen interactions with Trp 60, Asp 73, Leu 125, Ser 129, and π-π stacking with Tyr 47, Trp 88, Phe 101 residues. Ligand Nu.2 displayed hydrogen bonding with Tyr 56, Tyr 64, Asp 65, Thr 75, Ser 129, and π-π interactions with Tyr 47, Tyr 64. Ligand Nu.3 interacted with enzyme through hydrogen interactions with Tyr 56, Asp 73, Asp 73, Ser 129 and π-π stacking with Tyr 47, Trp 88, Phe 129, Ligand Nu.4 showed hydrogen interactions with Tyr 56, Trp 60, Asp 73, Leu 110 and π-π stacking wyr 64. Finally, ligand Nu.5 revealed hydrogen bonding with Tyr 56, Trp 60, Arg 61, Asp 73, Ser 129 and π-π interactions with Tyr 47 and Tyr 64. By investigating the interactions between the top five ligands and active site of the protein, it can be revealed that the presence of thiophene and benzene rings for π-π stacking interaction with Tyr 64 and Trp 47 and urea group to interact with ASP 73, Ser 129 and Tyr 56 residues have an effective role in increasing the affinity of compounds to the triphenyl-LasR protein. N-3-oxo-dodecanoyl homoserine lactone (3OC12-HSL) is a signaling molecule that activates LasR receptor function as a transcription factor and regulates biofilm expression formation. Tyr 56, Trp 60, Arg 61, Asp 73, and Ser 129 are essential residues engaged in hydrogen bond interactions between the triphenyl-LasR receptor and polar homoserine lactone head group (Zou and Nair, 2009). Among the five selected compounds, compounds Nu-8, Nu-9, and Nu-2 showed 4, 4 and 6 hydrogen bonds with the above residues, respectively, which indicates their high antagonist activity among other compounds to inhibit the protein (Fig. 4). The calculated free binding energy for these compounds was lower than -72 Kcal/mol. The free binding energy of the compound Nu (5) was the lowest (-94.75) (Table 2). We assessed the QSAR, ADME, and E-pharmacophore properties of these three selected ligands to select the best triphenyl-LasR inhibitory compound for further investigation.

3.3. Atom-based 3D-QSAR modeling

The atom-based QSAR approach study was carried out to evaluate the relationship between the structure and biological activity of three selected compounds. A dataset of 30 Transcriptional activator protein LasR inhibitors with their wide range of activities was used to build the QSAR model (Table 2). The significant model was obtained with the use of the third-PLS factor. Detailed statistics of the developed QSAR model have been reported in Table 2. The third PLS factor exhibited the best statistics for the training set compounds out of the three-PLS factor model. The model exhibited significant correlation coefficient (R^2 = 0.9943). The stability value was -0.0354, which shows the stability of the model prediction to the training set composition changes. The variance ratio (F value) was 1107.5, indicating the statistically significant regression model, and the smaller p-value (1.69E-021) indicated a greater degree of confidence. The reliability of the model was also expressed by a smaller standard deviation (SD= 0.0748), RMSE (0.95), and cross-validated correlation coefficient q^2 (-1.3629). Most of the statistical parameters were acceptable, indicating the developed 3D-QSAR model was a statistically significant and robust model. The plot of the predicted vs. experimental of the training and test sets compounds for the third PLS factor is shown in Fig. 5. The plot proved that the developed model had a good predictive ability.

3.3.1. Contour map analyses

The third validation obtained from 3D-QSAR was used to generate contour maps. These contour maps represent the positions that have a positive effect on bioactivity. We can gain the inhibitory activity by visualizing and understanding the maps against the most active and least active compounds. This could help us to discover novel scaffolds with good biological activity. The H-bond donor and hydrophobic contour map effects on the most dynamic and least active ligand were shown in Fig. 6. The contour map showed that the most active compound has the maximum favorable region (blue color for H-bond donor and green color for hydrophobic effect), and the least active compound has the leading unfavorable parts (red color for H-bond donor and yellow for hydrophobic effect).

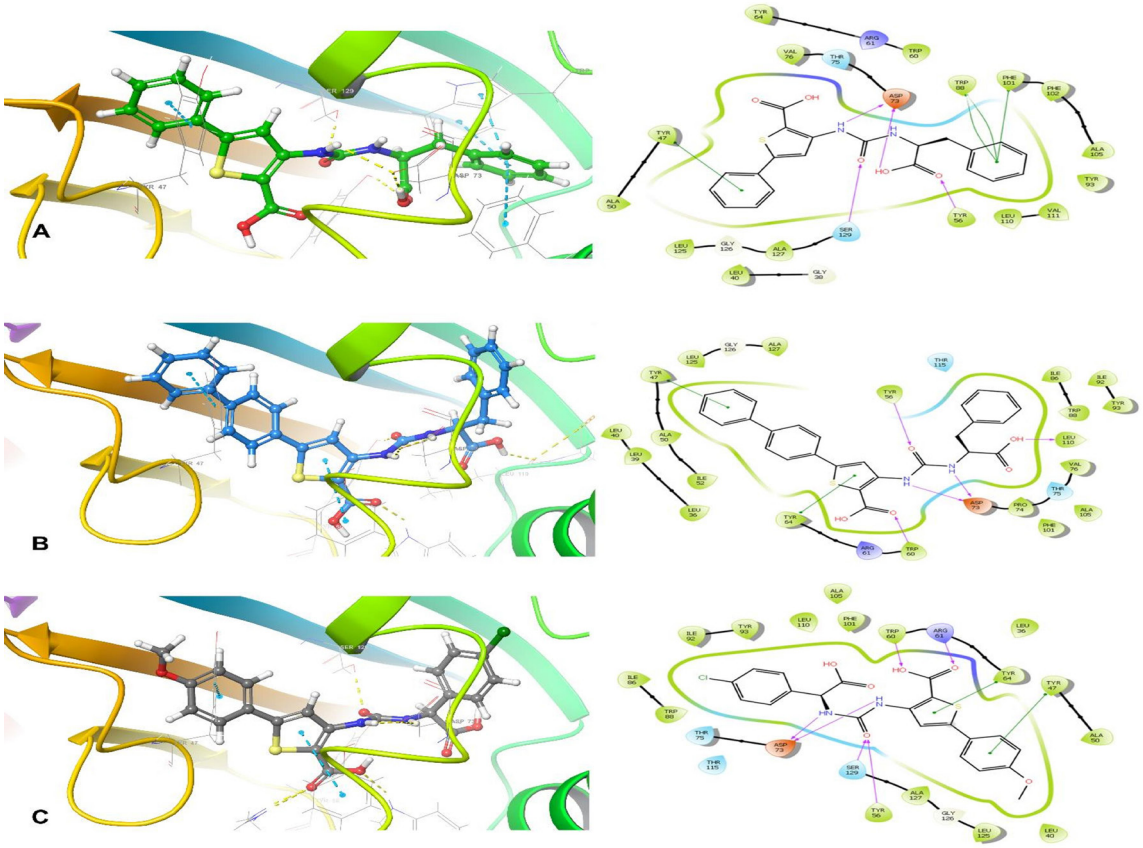

Fig. 4. Structure view and ligand interaction diagrams of the three selected ligands with PubChem ID (**A**) 118732847; (**B**) 118732854; and (**C**) 118732838 in complex with triphenyl-LasR protein.

Table 2
Statistical data for the QSAR model.

Factor	SD	R^2	R^2CV	R^2 Scramble	Stability	F	P	RMSE	Q^2	Pearson-r
1	0.3928	0.8269	-0.0028	0.8067	0.31	100.3	1.88E-09	0.98	-1.5175	-0.5813
2	0.1606	0.9725	-0.0385	0.9659	0.0283	353	2.52E-16	0.93	-1.2612	-0.4742
3	0.0748	0.9943	-0.0375	0.9902	-0.0354	1107.5	1.69E-21	0.95	-1.3629	-0.6293

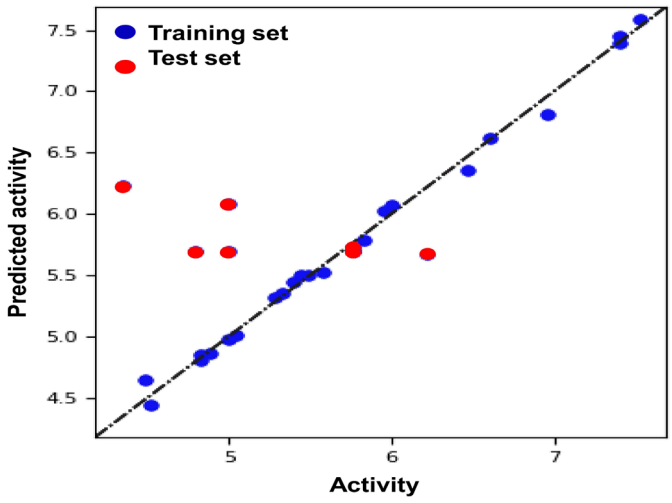

Fig. 5. Scatter plot of predicted and actual biological activity of the training and the test set.

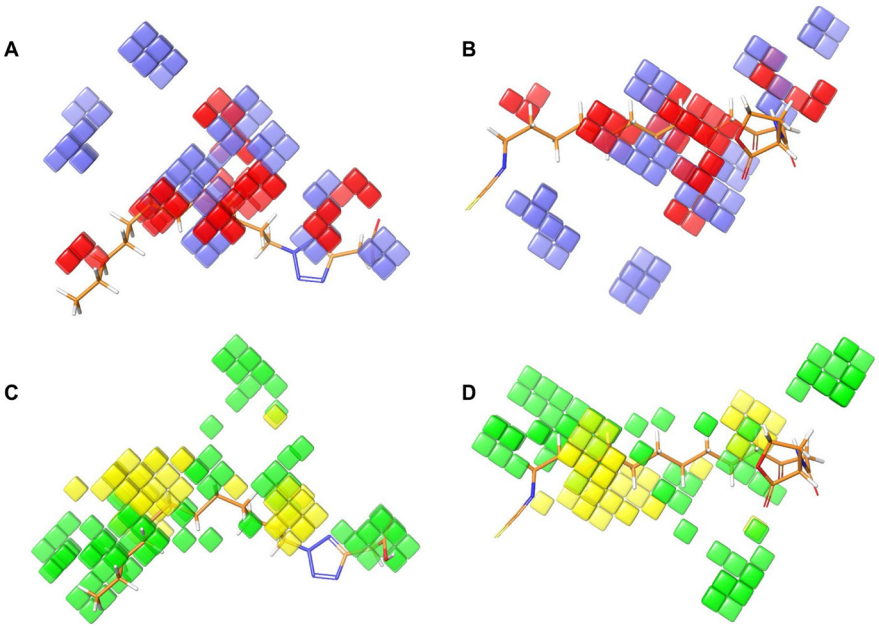

Fig. 6. H-bond donor effect (**A**) most active; (**B**) least active (blue, favorable; red, unfavorable); hydrophobic effect (**C**) most active; and (**D**) least active (green, favorable; yellow, unfavorable).

Hydrogen-bond donor mapping revealed that the ketone group, the nitrogen atom in the amide bond, and the hydroxyl group in the carboxylic functional group contributed favorably to the biological activity of compounds against the LasR enzyme. By investigating the predicted pIC_{50} of the most (= 7.52 µM) and least (= 4.34 µM) active compounds, it can be found that ligands Nu.2, Nu.9, and Nu.8 with predicted pIC_{50} 5.60, 5.69, and 5.77 µM, respectively, have one or more of these favorable groups that cause their good bioactivity.

3.4. Lipinski's rule for drug likeliness and in silico ADME prediction

The pharmaceutical properties of the three selected compounds were evaluated to study drug-likeness and predict the drug's pharmacokinetics, involving ADME (absorption, distribution, metabolism, and excretion) using QikProp module of the Schrodinger software. Oral bioavailability is one of the critical considerations for discovering and developing a new chemical entity (NCE) that should be investigated. All selected ligands showed oral absorption of more than 55%, while tobramycin showed no oral absorption. The other factors like MW, H-bond donors, acceptors, partition coefficient (QPlogPo/w), blood-brain barrier, and permeability (QPPCaco) were also calculated for the drug-like behavior of the selected compounds (Table 3). All the mentioned factors were in the allowed range indicating the high potential of selected ligands as a drug-like molecule. The statistical relationship between the variables for the three top-ranked ligands was investigated using a graph

Table 3
Qikprop Properties of Tobramycin and the top three compounds.

Ligand	PubChem ID	MW[a] (<500)	Donor HB (<5)	Accept HB (<10)	QPLogP$_o$/w[b] (-2 to 6.5)	Percent human oral absorption	QPPCaco[c] (<25 poor, >500 great)	QplogBB[d] (-3.0 to 1.2)	Rule of five (<4)
Nu-9	118732847	410.44	2.25	4.25	4.31	59.84	2.67	-2.23	0
Nu-8	118732854	486.54	2.25	4.25	5.99	56.93	2.75	-2.54	1
Nu-2	118732838	460.89	2.25	5	4.65	58.75	1.79	-2.4	0
Tobramycin	36294	467.518	15	20.3	-6.88	0	0.021	-3.44	2

[a]MW: Molecular weight; [b] LogP$_o$/w: Predicted octanol/water partition coefficient; [c] Predicted apparent Caco-2 cell permeability in nm/s; [d] logBB: Predicted brain/blood partition coefficient; Percentage of human oral absorption; Rule of five (no. of violations of Lipinski's rule of five: 0 is good and 4 is undesirable).

of the correlation matrix shown in Fig. 1. According to the matrix, the correlation of the QPlogPo/w is significantly related to MW. Also, the matrix shows that with increasing the MW and the number of violations of Lipinski's rule of five, the oral absorption decreases.

3.5. E-pharmacophore based virtual screening

According to the E-pharmacophore study on protein and native ligand complex, a seven-featured pharmacophore hypothesis ADHHRRR consists of one acceptor (A), one donor (D), two hydrophobic regions (H), and three aromatic rings (R) was generated (Fig. 7: A). To detect the best LasR inhibitor based on pharmacophore testing, three selected ligands were screened using this hypothesis and ranked in order of their fitness score (a measure of ligand alignment conformer matches the hypothesis based on RMSD site matching, vector alignments, and volume terms). Ligands Nu.2, Nu.9, and Nu.8 with hypothesis AADHRRR, ADRRR, and ADDRRRR showed fitness scores 1.62, 1.32, and 0.89, respectively. According to the native pharmacophore hypothesis, at least three aromatic rings, one amide bound and one halogen atom, are vital for the good binding affinity between ligand and protein. The hypothesis overlapping of each selected compound with the native ligand is shown in Fig. 7: B-D. Among the three selected ligands, the ligand with PubChem ID 118732838 has the highest fitness score (=1.62) and the closest pharmacophore hypothesis similarity (AADHRRR) with the native ligand. According to the obtained results from *in-silico* studies, we selected ligand with PubChem ID 118732838 as the potent triphenyl-LasR inhibitory that showed the potent desire with protein.

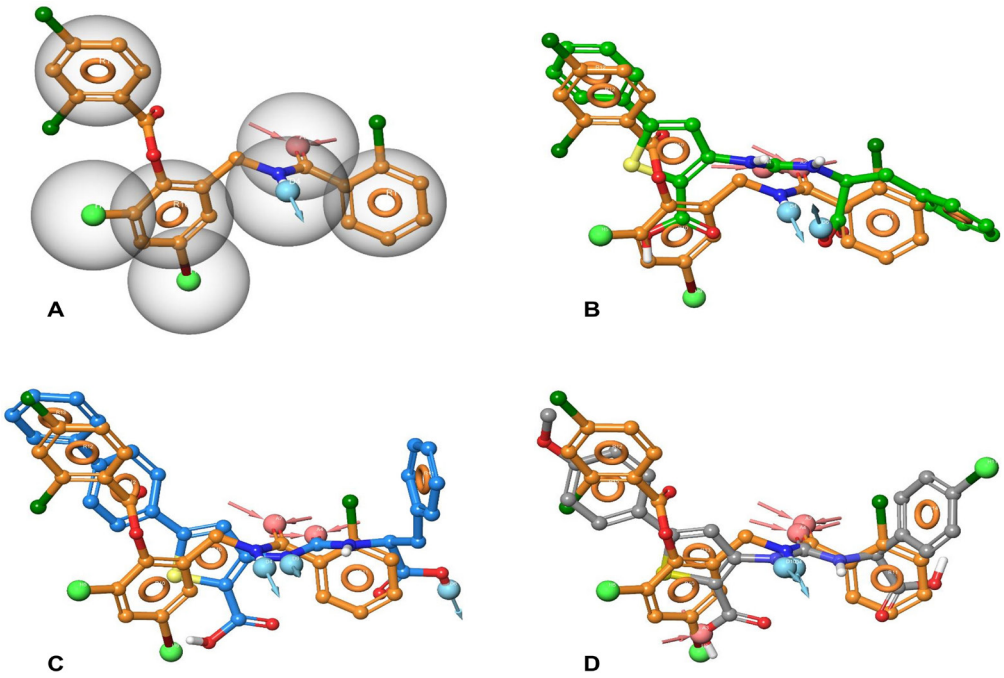

Fig. 7. (**A**) E-pharmacophore model (ADHHRRR) of the native ligand; Hypothesis overlapping of ligands with PubChem ID (**B**) 118732847; (**C**) 118732854; and (**D**) 118732838 with the native ligand

4. Concluding remarks

This study investigated the inhibitory activity of more than 700 (Half natural and half semi-synthesis) compounds against the triphenyl-LasR enzyme. The rigid receptor docking revealed the top ten ligands with glide scores in the range of -11.86 to -12.42 kcal/mol. For further investigations, the IFD study on the top ten compounds was performed. According to IFD scores and comparison of the ligand interaction between selected compounds and 3OC12-HSL, as an autoinducer, three ligands with PubChem ID: 118732847, 118732854, and 118732838 showed the highest binding potential with the protein that indicates their high inhibitory activity against the LasR system. These selected compounds were evaluated for QSAR and ADME studies to investigate their biological activity and drug-like behavior. The results indicated that all three compounds showed more than 55% oral absorption and had biological activity close to the most bioactive compound. The E-pharmacophore analysis was performed to investigate the pharmacophore features on the selected ligands that make key interactions. Comparison Fitness scores indicated that compounds with PubChem ID: 118732838 could be shown better interaction with the protein in comparison with the other ligands. Furthermore, it also showed the MM-GBSA score of -94.75 kcal/mol, indicating its high stability in the active pocket. According to the *in-silico* studies, a ligand with PubChem ID 118732838 was selected as the potent triphenyl-LasR inhibitory, which may be the potent candidate for suppressing the biofilm

formation and decrease the *P. aeruginosa* resistance.

Abbreviations

3D QSAR: 3D quantitative structure-activity relationship; ADME: Absorption, distribution, metabolism and excretion; AHL: Acyl-homoserine lactone; FDA: Food and Drug Administration; IFD: Induced fit ducking; MM-GBSA: Prime molecular mechanics-generalized born surface area; OPLS: optimized potentials for liquid simulations; PDB: Protein Data Bank; pIC_{50}: Negative logarithm of the IC_{50} value; QS: Quorum Sensing; XP mode: Extra precision mode.

Conflict of interest

The authors declare that there is no conflict of interest.

References

Akkerman-Nijland, A.M., Yousofi, M., Rottier, B.L., Van der Vaart, H., Burgerhof, J.G., Frijlink, H.W., Touw, D.J., Koppelman, G.H., Akkerman, O.W., 2020. Eradication of *Pseudomonas aeruginosa* in cystic fibrosis patients with inhalation of dry powder tobramycin. Ther. Adv. Respir. Dis. 14, 1753466620905279.

Al-Bagawi, A.H., Bayoumy, A.M., Ibrahim, M.A., 2020. Molecular modeling analyses for graphene functionalized with Fe_3O_4 and NiO. Heliyon 6(7), e04456.

Aliyu, A.B., Koorbanally, N.A., Moodley, B., Singh, P., Chenia, H.Y., 2016. Quorum sensing inhibitory potential and molecular docking studies of sesquiterpene lactones from *Vernonia blumeoides*. Phytochemistry 126, 23-33.

Chintha, C., Carlesso, A., Gorman, A.M., Samali, A., Eriksson, L.A., 2020. Molecular modeling provides a structural basis for PERK inhibitor selectivity towards RIPK1. RSC Adv. 10(1), 367-375.

de Kievit, T.R., Kakai, Y., Register, J.K., Pesci, E.C., Iglewski, B.H., 2002. Role of the *Pseudomonas aeruginosa* las and rhl quorum-sensing systems in rhlI regulation. FEMS Microbiol. Lett. 212(1), 101-106.

Fuqua, C., Greenberg, E.P., 2002. Listening in on bacteria: acyl-homoserine lactone signalling. Nat. Rev. Mol. Cell Biol. 3(9), 685-695.

Ganjoo, A., Prabhakar, C., 2019. *In silico* structural anatomization of spleen tyrosine kinase inhibitors: Pharmacophore modeling, 3D QSAR analysis and molecular docking studies. J. Mol. Struct. 1189, 102-111.

Gerdt, J.P., McInnis, C.E., Schell, T.L., Rossi, F.M., Blackwell, H.E., 2014. Mutational analysis of the quorum-sensing receptor LasR reveals interactions that govern activation and inhibition by nonlactone ligands. Chem. Biol. 21(10), 1361-1369.

Ho, D.K., Murgia, X., De Rossi, C., Christmann, R., Hüfner de Mello Martins, A.G., Koch, M., Andreas, A., Herrmann, J., Müller, R., Empting, M., 2020. Squalenyl hydrogen sulfate nanoparticles for simultaneous delivery of tobramycin and an alkylquinolone quorum sensing inhibitor enable the eradication of *P. aeruginosa* biofilm infections. Angew. Chem. - Int. Ed. 59(26), 10292-10296.

Kiratisin, P., Tucker, K.D., Passador, L., 2002. LasR, a transcriptional activator of P*seudomonas aeruginosa* virulence genes, functions as a multimer. J. Bacteriol. 184(17), 4912-4919.

Li, Z., Nair, S.K., 2012. Quorum sensing: how bacteria can coordinate activity and synchronize their response to external signals? Protein Sci. 21(10), 1403-1417.

Manson, D.E., O'Reilly, M.C., Nyffeler, K.E., Blackwell, H.E., 2020. Design, synthesis, and biochemical characterization of non-native antagonists of the *Pseudomonas aeruginosa* quorum sensing receptor LasR with nanomolar IC_{50} values. ACS Infect. Dis. 6(4), 649-661.

Mizdal, C.R., Stefanello, S.T., Nogara, P.A., Soares, F.A.A., de Lourenço Marques, L., de Campos, M.M.A., 2018. Molecular docking, and anti-biofilm activity of gold-complexed sulfonamides on *Pseudomonas aeruginosa*. Microb. Pathog. 125, 393-400.

Norouzi, S., Farahani, M., Nejad Ebrahimi, S., 2021. The integration of pharmacophore-based 3D QSAR modeling and virtual screening in identification of natural product inhibitors against SARS-CoV-2. Pharm. Sci.

O'Brien, K.T., Noto, J.G., Nichols-O'Neill, L., Perez, L.J., 2015. Potent irreversible inhibitors of LasR quorum sensing in *Pseudomonas aeruginosa*. ACS Med. Chem. Lett. 6(2), 162-167.

Pejin, B., Ciric, A., Dimitric Markovic, J., Glamoclija, J., Nikolic, M., Sokovic, M., 2017. An insight into anti-biofilm and anti-quorum sensing activities of the selected anthocyanidins: The case study of Pseudomonas aeruginosa PAO1. Nat. Prod. Res. 31(10), 1177-1180.

Pejin, B., Ciric, A., Glamoclija, J., Nikolic, M., Sokovic, M., 2015a. *In vitro* anti-quorum sensing activity of phytol. Nat. Prod. Res. 29(4), 374-377.

Pejin, B., Ciric, A., Glamoclija, J., Nikolic, M., Stanimirovic, B., Sokovic, M., 2015b. Quercetin potently reduces biofilm formation of the strain *Pseudomonas aeruginosa* PAO1 *in vitro*. Curr. Pharm. Biotechnol. 16(8), 733-737.

Pejin, B., Iodice, C., Tommonaro, G., Stanimirovic, B., Ciric, A., Glamoclija, J., Nikolic, M., De Rosa, S., Sokovic, M., 2014. Further *in vitro* evaluation of antimicrobial activity of the marine sesquiterpene hydroquinone avarol. Curr. Pharm. Biotechnol. 15(6), 583-588.

Subhani, S., Jamil, K., 2015. Molecular docking of chemotherapeutic agents to CYP3A4 in non-small cell lung cancer. Biomed. Pharmacother. 73, 65-74.

Vora, J., Patel, S., Sinha, S., Sharma, S., Srivastava, A., Chhabria, M., Shrivastava, N., 2019. Molecular docking, QSAR and ADMET based mining of natural compounds against prime targets of HIV. J. Biomol. Struct. Dyn. 37(1), 131-146.

Zou, Y., Nair, S.K., 2009. Molecular basis for the recognition of structurally distinct autoinducer mimics by the *Pseudomonas aeruginosa* LasR quorum-sensing signaling receptor. Cell Chem. Biol. 16(9), 961-970.